Analysis of transport in gyrokinetic tokamaks*

H. E. Mynick† and S. E. Parker
Plasma Physics Laboratory, Princeton University, P.O. Box 451, Princeton, New Jersey 08543-0451

(Received 14 November 1994; accepted 24 January 1995)

Progress toward a detailed understanding of the transport in full-volume gyrokinetic simulations of tokamaks is described. The transition between the two asymptotic regimes (large and small) of scaling of the heat flux with system size a/ρ_g reported earlier is explained, along with the approximate size at which the transition occurs. The larger systems have transport close to that predicted by the simple standard estimates for transport by drift-wave turbulence (viz., Bohm or gyro-Bohm) in scaling with a/ρ_g, temperature, magnetic field, ion mass, safety factor, and minor radius, but lying much closer to Bohm, which seems the result better supported theoretically. The characteristic downshift in the $\langle k_\theta \rangle$ spectrum observed previously in going from the linear to the turbulent phase is consistent with the numerically inferred coupling coefficients M_{kpq} of a reduced description of the system. An explanation of the downshift is given from the resemblance of the reduced system to the Hasegawa–Mima or Terry–Horton systems. These manifest an analogous downshift in slab geometry, and have M_{kpq} resembling those inferred from the gyrokinetic (GK) data. © *1995 American Institute of Physics.*

I. INTRODUCTION

In recent work[1] we have initiated a study analyzing the transport in full-volume gyrokinetic (GK) simulations of tokamaks. The considerable resemblance of these systems to real experiments makes an understanding of their transport highly relevant, while their far greater simplicity should make the development of a reliable first-principles transport theory for them more attainable. In the present paper, we discuss further progress we have made toward this objective, including additional insight gained into results only reported earlier.

In Ref. 1, we followed two complementary lines of investigation, analogous to what has been done for real experiments: (1) a "top-down" approach, studying the scalings of transport with important plasma parameters, including system size a/ρ_g (ρ_g is the ion gyroradius), temperature T, magnetic field strength B, ion mass M, safety factor q, and minor radius r; and (2) a "bottom-up" approach, toward developing a first-principles theory of the transport. Here, we continue the development of both lines of study.

II. TRANSPORT SCALINGS

In Ref. 1 a power-law scaling of the conductivity $\chi \sim q^x T^y B^z M^w$ modeling the transport physics was assumed, and the exponents x, y, z, and w inferred from parameter scans of GK runs, and compared with their values from two analytic estimates [viz., Bohm and gyro-Bohm (gB)] and two experimental scalings [viz., "Low" (L) or "High" (H) mode, and supershots]. Scaling arguments[2] for these electrostatic collisionless simulations were invoked to determine two of the exponents $[z \to (1-2y), w \to (y-1)]$ for the GK systems, leaving only two independent exponents x and y, determined by GK runs. Summarizing the scalings found are Table I, along with Figs. 1 and 2. These improve and extend the results given in the analogous table and figures (Figs. 17 and 15, respectively) in Ref. 1 in respects indicated below. The figures summarize the results of the parameter scans for y (scaling with a/ρ_g) and x (scaling with q_a), respectively. In Ref. 1, all runs (except the $a/\rho_g = 128$ case) were done without the four-point gyroaverage.[3] Particle gyroaveraging will reduce the level of the heat flux due to orbit averaging, but this effect should be small, since the steady-state spectrum peaks in a range of small $k_\perp \rho_i$ and, moreover, should affect different runs in a similar way. All runs shown in Fig. 1 here have been done with the four-point gyroaveraging. The scaling results from Fig. 1 here and Fig. 17 in Ref. 1 are almost unchanged, confirming this expectation.

Two regimes of scaling were found (Fig. 1): one for "small" GK systems (gk-s scaling), having $a/\rho_g < 64$ for the assumed background profiles, and another for "large" systems (gk-l scaling), with $a/\rho_g > 64$. The dotted and dashed guidelines show the location of Bohm ($y = y_B = 1$) and gyro-Bohm ($y = y_{gB} = 1.5$) scalings. It was found that small GK systems have values of x, y, and w close to those of supershots, hence, similar scalings in q_a (or current I_p), T (or power P), and M, but scale quite differently with B. It was noted that this resemblance was probably only coincidental, since supershots in the Tokamak Fusion Test Reactor (TFTR)[4] have $a/\rho_g \sim 500$ and $T_i/T_e \gg 1$, while the gk-s simulations have $a/\rho_g \lesssim 64$ and used $T_i = T_e$. There, no reason was given for the origin of the scaling, and, in particular, for the value $y \simeq 0$, which implies that the heat flux $Q \propto (a/\rho_g)^{1-2y}$ falls off as the system size diminishes, in contrast to the trend for large systems. The large- to small-system transition can be qualitatively understood as follows. The ion temperature gradient (ITG) instabilities that produce the turbulence in these simulations yield a saturated spectrum peaking around[5] $k_\theta \rho_g \simeq 0.15$, and for a given toroidal mode number n have a dominant poloidal mode number m, given approximately by $m \simeq q(r)n$. Taking the surface $r = r_0$ where the temperature gradient peaks equal to $a/2$ and $q(r_0) = 2$, as in the simulations for this parameter scan, one

*Paper 5IA1, Bull. Am. Phys. Soc. **39**, 1637 (1994).
†Invited speaker.

TABLE I. Transport scalings.

Scaling	x,y,z,w	$\chi \sim q^x T^y B^z M^w$	τ_E
Analytic/numerical:			
gk-s	0.25,−0.1,1.2,−1.1	$q^{0.25}T^{-0.1}B^{1.2}M^{-1.1}$	$P^{0.1}B^{-1.6}I_p^{0.28}M^{1.2}$
Bohm	0,1,−1,0	$q^0T^1B^{-1}M^0$	$P^{-0.5}B^{0.5}I_p^0M^0$
gk-l	0.25,1.1,−1.2,0.1	$q^{0.25}T^{1.1}B^{-1.2}M^{0.1}$	$P^{-0.5}B^{0.45}I_p^{0.12}M^{0.05}$
gB	0,1.5,−2,0.5	$q^0T^{1.5}B^{-2}M^{0.5}$	$P^{-0.6}B^{0.8}I_p^0M^{-0.2}$
Experimental:			
L,H mode	2,1,−2,−1	$q^2T^1B^{-2}M^{-1}$	$P^{-0.5}B^0I_p^1M^{0.5}$
Supershot	0,0,−0.6,−0.8	$q^0T^0B^{-0.6}M^{-0.8}$	$P^0B^{0.6}I_p^0M^{0.8}$

has $k_\theta\rho_g = 2m\rho_g/a \simeq 4n\rho_g/a$. Thus, as a/ρ_g decreases, $m(r_0)$ and n must decrease in order to keep $k_\theta\rho_g$ constant, so that below $a/\rho_g = 4/0.15 \simeq 27$, even $n=1$ does not yield a small enough k_θ to capture this spectral peak. Actually, one needs $n \gtrsim 2$ at the peak, in order to permit the presence of other, lower-k_θ modes important in larger systems in allowing for a multimode system rather than one dominated by a single coherent mode. Thus, one expects a significant loss of modes contributing to transport, and a concomitant reduction of transport levels, for systems smaller than $a/\rho_g \simeq 54$, consistent with the transition from the gk-l to the gk-s-scalings observed in Ref. 1.

Large GK systems manifest scalings close to the Bohm expression $\chi_B = cT/eB$ in scaling with system size a/ρ_g, and hence with T, B, and M, as well as with $q_a \equiv q(r=a)$ and r. A rough theoretical basis exists for this scaling as well. We first recall the mixing-length arguments, from which either χ_B or the gyro-Bohm expression $\chi_{gB} \simeq \kappa\rho_g\chi_B$ can be derived. [Here, $\kappa = -\partial_r \ln f_0$ is the inverse of the radial scale length of the background distribution f_0. In the runs in Ref. 1, which had density gradient $n_0' = 0$, one has $\kappa = \kappa_T$, with $\kappa_T(r) \equiv L_T^{-1}(r)$ the inverse temperature gradient scale length, peaking at $r = r_0$.] One has $\chi \sim \gamma/k_r^2$, with $\gamma \sim \omega_* = -k_\theta \kappa cT/(eB)$. Thus, $\chi \sim \chi_B(\kappa k_\theta/k_r^2)$, with $k_\theta \sim \rho_g^{-1}$ and the replacements $k_r \to k_\theta$ for χ_{gB} and $k_r^2 \to k_\theta\kappa$ for χ_B. Linear theory for toroidal drift-type modes indicates[6,7] that the slow radial variation of the profiles produces linear modes with radial extent $\lambda_r \sim \sqrt{\rho_g L_T}$, i.e., roughly with the replacement $k_r^2 \to k_\theta\kappa$ needed for Bohm scaling. Thus, while the chain of arguments involved is in several places somewhat crude, the foregoing discussion provides a coherent picture for both the observed regimes of GK scaling.

Enhancing this picture is insight into the radial scaling of Q or χ. A significant difference between the GK tokamaks and real machines is that for the former, the modes are radially global, but local in the latter. Adopting the Bohm expression for k_r above, one expects the k_r spectrum to have a width $\langle k_r\rho_g\rangle = c_r\sqrt{\rho_g/a}$, with c_r a numerical factor, which we fix by the GK data. As shown in Ref. 1, for $\rho_g/a = \frac{1}{64}$, one finds $\langle k_r\rho_g\rangle \simeq 0.2$, implying $c_r \simeq 1.6$. Thus, $a/\lambda_r \simeq \langle k_r a\rangle/2\pi \simeq (c_r/2\pi)\sqrt{a/\rho_g} \simeq 2$. For TFTR, however, for which $a/\rho_g \simeq 500$, one has instead $a/\lambda_r \simeq 6$. Thus, since $a/\lambda_r \simeq 2$ is of order unity for the GK simulations, as noted in Ref. 1 the radial variation of Q should be determined by the radial profiles of the global modes present, consistent with the numerical findings presented in Ref. 1. For real machines, where $a/\lambda_r \simeq 6$ allows many modes across the minor radius, consistent with the more standard picture one expects $Q(r)$ to instead derive from the radial variation of $\gamma/k_\perp^2$ for modes localized at different radii. It has been pointed out[8–10]

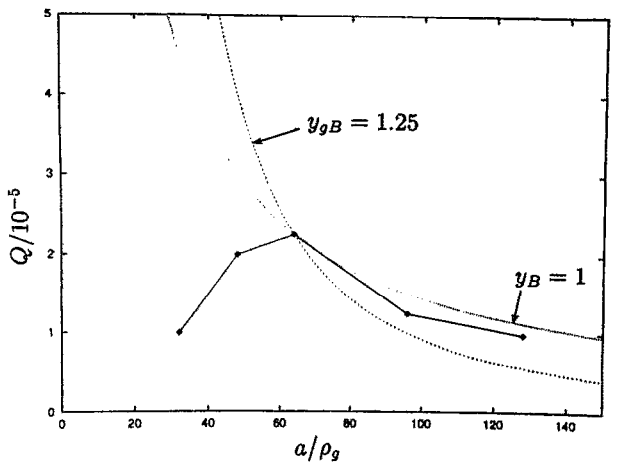

FIG. 1. Scaling of Q with a/ρ_g, with $q_0 = 1.25$ and $q_a = 4.25$.

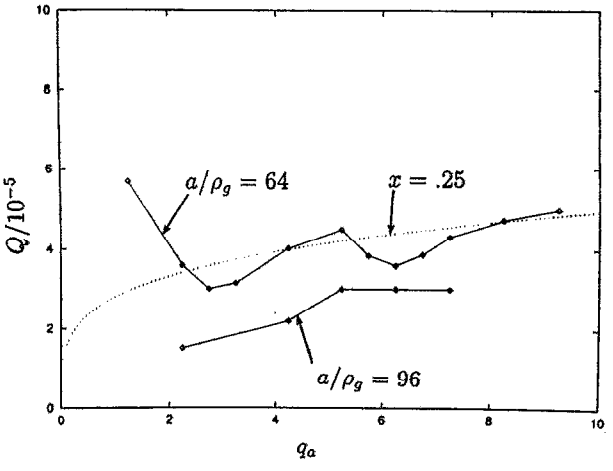

FIG. 2. Parameter scan of heat flux Q vs q_a, for GK tokamaks with $q_0 = 1.25$, for $a/\rho_g = 64$ and 96.

that critical-gradient models, in which χ_{gB} in the assumed expression for χ is enhanced by a factor $\sim(R/L_T - R/L_{T\,crit})$ of the distance above the threshold, can reproduce the experimentally observed rise of χ as $r\to a$ (contrary to what is predicted using χ_{gB} or χ_B alone), while retaining a gyro-Bohm or Bohm-like global scaling with a/ρ_g. Using χ_B instead of χ_{gB} produces a model that agrees as well or better with experiment.[11] For simulations where $a/\lambda_r\sim 1$, a radial variation of $(R/L_T - R/L_{T\,crit})$ could have a similar effect on $Q(r)$ as for the local-mode mechanism, by shifting the maximum position of the individual mode profiles toward the outside, from the symmetrically centered form of the present simulations, which produce a $Q(r)$ consistent with the simple Bohm or gyro-Bohm expressions.[1]

In Ref. 1 it was speculated that, while the q_a scan at $a/\rho_g=64$ exhibited only a gentle increase with q_a ($x=0.25$), far below the L- or H-mode value of $x=2$, perhaps this exponent would increase toward that experimental value for larger a/ρ_g. Further investigation suggests that this is not the case. In Fig. 2 is shown both the results from the same scan at $a/\rho_g=64$ presented in Ref. 1, plus a less complete scan at $a/\rho_g=96$. One sees that the rise with increasing q_a is at least as weak as in the smaller systems, retaining the closeness of the GK exponents to those of the Bohm expression. The weaker q scaling for the GK systems may be due to a number of factors. The current simulations have no trapped electron drive, and so are missing the stronger q dependences, which it has been argued[12,13] should be present for trapped-electron modes. They also have a large aspect ratio, implying few trapped ions, and relatively strong ITG growth rates, so that trapped ion modes should be unimportant for them. Were they important, as they might be in real machines, one would again expect a stronger q scaling for χ, making the heuristic replacement $\lambda_r\sim\sqrt{\rho_g L_T}\to\sqrt{\rho_b L_T}\sim q^{1/2}\rho_g L_T$ in the scaling arguments sketched earlier. (Here, ρ_b is the ion banana width.) The oscillatory character observed earlier in the $a/\rho_g=64$ curve is not apparent in that for $a/\rho_g=96$. This may be due only to the less complete scan represented there, or to the fact that individual rational surfaces and their corresponding modes are not important in larger systems with a wider range of excited modes.

III. NONLINEAR PHYSICS

In Ref. 1, the method of Ritz *et al.*[14] was used to infer the linear coefficients $L_k\equiv -i\omega_k\equiv(\gamma_k - i\omega_{rk})$ and nonlinear coupling coefficients M_{kpq} in the mode coupling equation,

$$\partial_t\phi_k = L_k\phi_k + \frac{1}{2}\sum_{0=k+p+q} M_{kpq}\phi_p^*\phi_q^*, \tag{1}$$

for a reduced set of only a few tens of harmonics k, which the GK data indicated contained the essential transport physics. The inferred M_{kpq} were then used to infer the rate of nonlinear power transfer between modes, and found consistent with a downshift observed in the $\langle k_\theta\rangle$ spectrum in going from the linear to the nonlinear phase, peaking around $n=4$ in the linear phase, and at 2 nonlinearly. However, the reason for the downshift was not addressed. It appears that this may be understood from a resemblance of the present toroidal

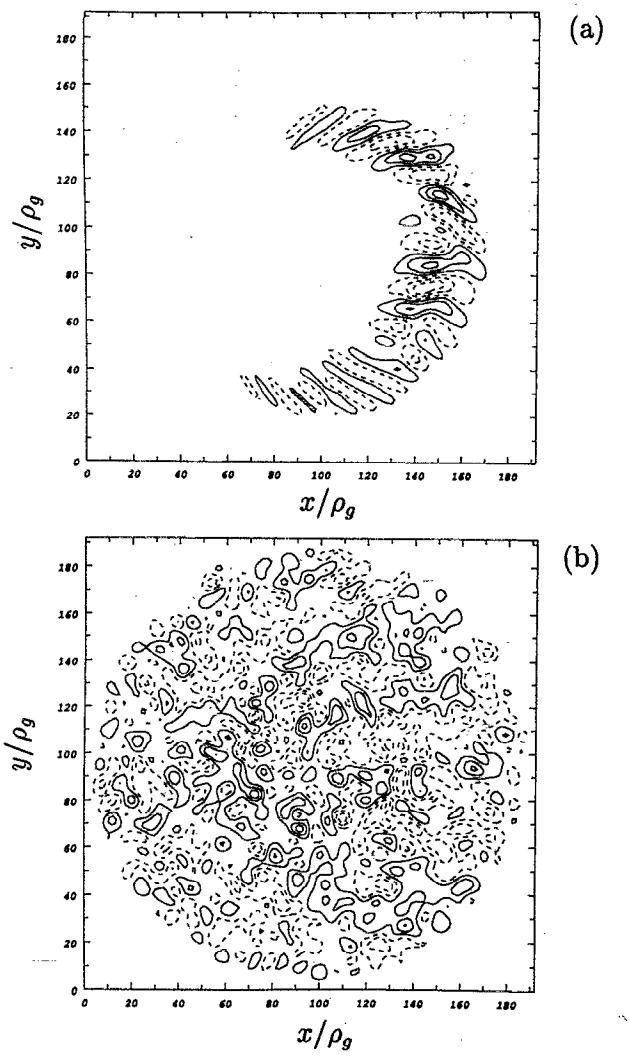

FIG. 3. Contours of constant potential for (a) the linear growth phase and (b) the quasisteady saturated phase of a GK run.

problem with what occurs in the slab Hasegawa–Mima[15] (HM) or Terry–Horton[16] (TH) problems. In Ref. 16, simulating the TH equation for a minimal set of 20 modes k (ten modes plus complex conjugates), Terry and Horton point out the isotropizing effect of the M_{kpq}, redistributing power from modes with smaller k_x and larger k_y, where the most unstable modes lie, toward larger k_x and smaller k_y. A similar redistribution of power occurs in the HM equation. The approximate correspondence of the slab to the toroidal wave vectors is $(k_x,k_y)\to(k_r,k_\theta)$. Thus, the downshift in $\langle k_y\rangle$ in Ref. 16 corresponds to a downshift in $\langle k_\theta\rangle$, as observed in the toroidal GK simulations. If this correspondence is valid, then the GK simulations should also manifest an upshift in $\langle k_r\rangle$. Comparing the typical radial scale in Figs. 3(a) (linear phase) and 3(b) (nonlinearly saturated phase), one notes that the $\langle k_r\rangle$ upshift also appears to occur. One would also expect the inferred M_{kpq} to resemble the HM coefficients $M_{kpq}^{HM} = w_{pq}(q^2 - p^2)/(1 + k^2)$ [with $w_{pq}\equiv(c/B)\hat{\mathbf{b}}\cdot\mathbf{p}\times\mathbf{q}$]. Computing these requires knowing k_r for the modes of the system, which up to now have been labeled only by n and m on

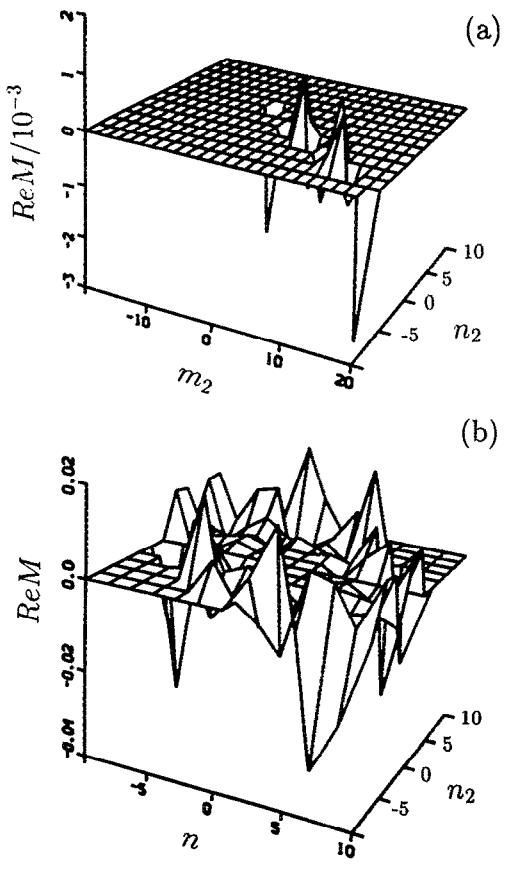

FIG. 4. Plots of the Hasegawa–Mima coupling coefficients M_{kpq}^{HM} for the reduced 32-mode system of Ref. 1. (a) M_{kpq}^{HM} over the $\mathbf{p}\equiv(m_2,n_2)$ plane, for fixed $\mathbf{k}\equiv(m,n)=(10,5)$. (b) M_{kpq}^{HM} over the n, n_2 plane.

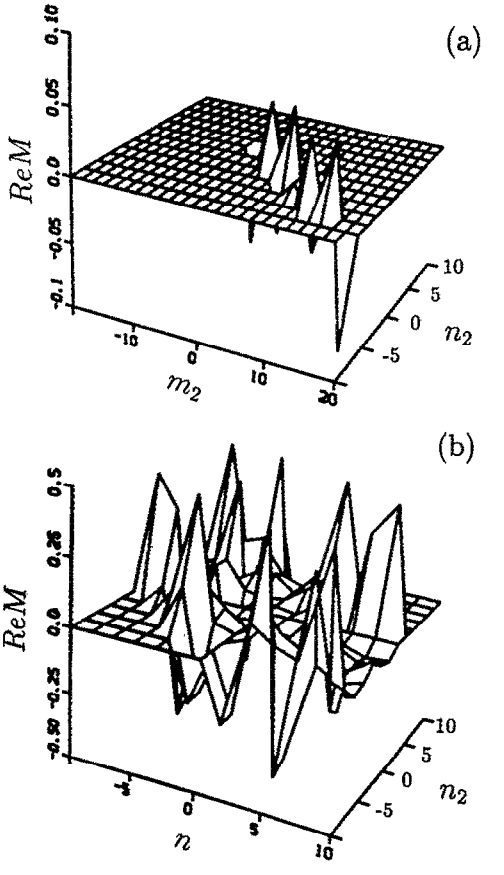

FIG. 5. The same as for Fig. 4, but for the numerically inferred M_{kpq}.

the flux surface of observation $r=r_0$. For the results shown here, we use a method for inferring these, which is somewhat crude, but has the virtue that it only requires data from $r=r_0$, on the basis of which the mode selection, and the inference of the L's and M's was carried out in Ref. 1. A refined approach, using data from many surfaces, is now under development. Using the single-surface method, in Fig. 4 we display M_{kpq}^{HM} for the 32 modes of the reduced system. In (a), these are plotted over the $\mathbf{p}=(m_2,n_2)$ plane, for $\mathbf{k}=(10,5)$. Because the modes of the system, all lie in the nearly one-dimensional (1-D) locus where $k_{\|}\simeq 0$, one can approximately represent $\mathbf{k}$ and $\mathbf{p}$ by just their n values n and n_2, and so display all the M_{kpq} of the system over the (n,n_2) plane. This is shown in Fig. 4(b). This may be compared with the analogous plots for the inferred coefficients in Fig. 5. One notes the considerable resemblance. Both composite plots, Figs. 4(b) and 5(b), manifest the same hollow, bowl-like form, with a scalloped edge of peaks and troughs. One sees from Fig. 4(a) that the M_{kpq}^{HM} have only a small number of peaks ($N_p\sim 5$) along the $p_{\|}\simeq 0$ line, the same as the inferred M_{kpq} in Fig. 5(a), which provided one of the simplifications in Ref. 1 for a reduced description of the essential transport physics. For the M_{kpq}^{HM}, this occurs largely due to the factor w_{pq} in M_{kpq}^{HM}. The bowl-like form exhibited in Fig. 4(b) comes both from w_{pq} and the factor $(q^2-p^2)/(1+k^2)$, both of which become small as $k\equiv|\mathbf{k}|$, $p\equiv|\mathbf{p}|$, and $q\equiv|\mathbf{q}|$ do.

The most notable difference between the two is that the inferred coefficients are larger than those from the HM equation by a factor of about 20. It has been suggested[17] that such an enhancement is what one might have expected, because in the nonlinearity $\mathbf{v}_E\cdot\nabla\delta n$ for the HM equation [with $\delta n=(1-\nabla_{\perp}^2)\phi$], the lowest-order (in powers of k, p, and q) "$E\times B$" portion $\sim\hat{\mathbf{b}}\times\nabla\phi\cdot\nabla\phi$ vanishes, leaving only the $\mathcal{O}(k^2)$ "polarization" portion $\sim\hat{\mathbf{b}}\times\nabla\phi\cdot\nabla\nabla^2\phi$. In contrast, for ITG turbulence, the lowest-order part of the nonlinearity $\mathbf{v}_E\cdot\nabla\delta p$ in the pressure equation survives, making the (appropriately scaled) nonlinearity larger than for the HM nonlinearity by $\sim 1/k^2\sim 1/(0.15)^2\simeq 44$, of size comparable to the observed enhancement. However, still needed is a fuller analytic calculation of the toroidal M_{kpq}, which could establish the validity of this argument, and make more precise predictions on the expected form and scalings.

The resemblance of the inferred M_{kpq} to the M_{kpq}^{HM} may be useful in computing the nonlinearly saturated spectrum of the ϕ_k from the reduced system description. As noted in Ref. 1, even small inaccuracies in the M_{kpq} (as well as in the L_k) can introduce spurious growth rates, seriously distorting the character of the saturated spectrum, and so the predicted transport. Even for the test data on which the inference method was benchmarked in Ref. 1, where the statistics (number of realizations $N_{\mathrm{rl}}=2000$) provided good agreement

between the real $[L,M]$ generating the data and the inferred values, an integration of Eq. (1) using the inferred coefficients produces a noticeable deviation after only a fraction of the time of the GK simulations. The statistics provided by the test data is a good deal better than is computationally accessible for the GK data. Thus, to obtain a description $[L,M]$ accurate enough to correctly predict the saturated GK spectrum, the presently inferred coefficients probably cannot be used directly, but may be used as a guide for analytic calculations, which will be more likely to maintain important symmetries or conservation laws whose violation might cause spurious results. The comparison of the inferred M_{kpq} with the M_{kpq}^{HM} shown here may be viewed as a first step in that process.

IV. DISCUSSION

A number of elements of a theoretical understanding of the transport in the GK tokamaks being simulated here (viz., with electrostatic fluctuations only, adiabatic electrons, and collisionless ions) seem to be emerging. We have seen that these systems exhibit two regimes of scaling: one for smaller systems and one for larger ones, of which the latter (for the profiles employed here, for $a/\rho_g > 64$) is the more relevant experimentally. The large systems display scalings (with r, with q_a, and with a/ρ_g, hence, also with T, B, and M), which are close to those given by the Bohm expression χ_{B}, falling off as $Q \propto (a/\rho_g)^{-1}$ as a/ρ_g increases. Rough arguments have been presented for the transition below $a/\rho_g \simeq 64$ to the small-system behavior $Q \propto a/\rho_g$, as well as to the a/ρ_g value at which the transition occurs. The Bohm scaling may also be theoretically obtained, albeit crudely, by the usual mixing-length arguments, supplemented by arguments from linear theory on the scaling of $\langle k_r \rangle$ with system size, arguments supported by the observed GK spectrum.[1]

These approximate arguments must now be supported by the more fundamental theory represented by the reduced description of the transport physics. The M_{kpq} numerically inferred for this description predict the nonlinear downshift in the $\langle k_\theta \rangle$ spectrum earlier observed in the simulations in going from the linear to the nonlinear saturated phase, and an explanation has been given for the downshift as due to the resemblance of this toroidal problem to the slab problems of the Hasegawa–Mima and Terry–Horton equations. This picture is supported by the $\langle k_\theta \rangle$ downshift, by an accompanying upshift in $\langle k_r \rangle$, and by a marked resemblance of the M_{kpq} inferred from the data with the M_{kpq}^{HM}.

Using the inferred M_{kpq} as a guide, an analytic calculation of the toroidal M_{kpq} now is needed, to complete a theoretical derivation of the reduced description, from which the saturated spectrum might be predicted (and from this the transport), without spurious effects introduced by the statistical limitations on the GK data.

ACKNOWLEDGMENTS

We are grateful to J. C. Cummings for his help in generating Fig. 3, and to G. W. Hammett, J. A. Krommes, and W. W. Lee for useful discussions.

Computing resources provided by the National Energy Research Supercomputing Center and the Pittsburgh Supercomputing Center. This work was supported by the U.S. Department of Energy, Contract No. DE-AC02-76-CHO3073.

[1] H. E. Mynick and S. E. Parker, Phys. Plasmas **2**, 1217 (1995).
[2] J. W. Connor and J. B. Taylor, Nucl. Fusion **17**, 1047 (1977).
[3] W. W. Lee, J. Comput. Phys. **72**, 243 (1987).
[4] D. J. Grove and D. M. Meade, Nucl. Fusion **25**, 1167 (1985).
[5] S. E. Parker, W. W. Lee, and R. A. Santoro, Phys. Rev. Lett. **71**, 2042 (1993).
[6] D. I. Choi and W. Horton, Phys. Fluids **23**, 356 (1980).
[7] S. C. Cowley, R. M. Kulsrud, and R. Sudan, Phys. Fluids B **3**, 2767 (1991).
[8] G. Bateman, Phys. Fluids B **4**, 634 (1992).
[9] D. D. Hua, X. Q. Xu, and T. K. Fowler, Phys. Fluids B **4**, 3216 (1992).
[10] W. Dorland, M. Kotschenreuther, M. A. Beer, G. W. Hammett, R. E. Waltz, R. R. Dominguez, P. M. Valanju, W. H. Miner, J. Q. Dong, W. Horton, F. L. Waelbroeck, T. Tajima, and M. J. LeBrun, *Proceedings of the 15th International Conference on Plasma Physics and Controlled Nuclear Fusion Research*, Seville, Spain, 1994 (International Atomic Energy Agency, Vienna, 1995), Paper IAEA-CN-60/D-P-I-6.
[11] W. Dorland (private communications, 1994).
[12] W. M. Tang, in *Theory of Fusion Plasmas*, Proceedings of the Joint Varenna–Lausanne International Workshop, Varenna, Italy 1990, edited by J. Vaclavik, F. Troyon, and E. Sindoni (Editrice Compositori, Bologna, 1990), pp. 31–44.
[13] H. E. Mynick and S. J. Zweben, Nucl. Fusion **32**, 518 (1992).
[14] Ch. P. Ritz, E. J. Powers, and R. D. Bengston, Phys. Fluids B **1**, 153 (1989).
[15] A. Hasegawa and K. Mima, Phys. Rev. Lett. **39**, 205 (1977).
[16] P. W. Terry and W. Horton, Phys. Fluids **26**, 106 (1983).
[17] G. W. Hammett (private communications, 1994).